Supporting information for "Effects of iron spin transition on the structure and stability of large primordial reservoirs in Earth's lower mantle"

Yang Li[1,2,3], Kenny Vilella[4], Frédéric Deschamps[4], Liang Zhao[1,2,3],Paul J.Tackley[5]

Contents of this file

1. Text S1: Numerical model set-up
2. Figure S1: Snapshots of composition and temperature fields for different cases
3. Table S1: Parameters of the numerical models

Introduction

This supporting information file provides a detailed description of numerical models used in this study (see text S1), and the parameters of the numerical models (see Table S1).

Text S1: Numerical model set-up

We conducted numerical simulations of thermo-chemical convection using the code StagYY [*Tackley*, 2008] modified to include the density tables calculated, following the

---

Correspondence to: Yang Li(yli@mail.iggcas.ac.cn) and Kenny Vilella (vilella@earth.sinica.edu.tw).

[1]State Key Laboratory of Lithospheric

method developed by *Vilella et al.* [2015] (section 2.1 in the main text). StagYY solves the conservation equations of mass, momentum, energy, and composition for an anelastic compressible fluid with infinite Prandtl number. Same to those in *Vilella et al.* [2015], the governing equations are:

conservation of mass

$$\nabla \cdot (\rho \underline{v}) = 0 \tag{1}$$

Evolution, Institute of Geology and Geophysics, Chinese Academy of Sciences, Beijing, China

[2]Institutions of Earth Science, Chinese Academy of Sciences, Beijing, China

[3]Laboratory for Marine Mineral Resources, Qingdao National Laboratory for Marine Science and Technology, Qingdao, China

[4]Institute of Earth Sciences, Academia Sinica, Taipei, Taiwan

[5]Institute of Geophysics, Department of Earth Sciences, ETH Zurich, Zurich, Switzerland

momentum

$$\underline{\nabla} \cdot \underline{\underline{\sigma}} - \underline{\nabla} p = \frac{Ra \cdot \Delta\rho_{model} \cdot \widehat{\underline{r}}}{\Delta\rho_{th}} \tag{2}$$

and energy

$$\rho C_p \frac{DT}{Dt} = -Di_S \alpha \rho T v_r + \underline{\nabla} \cdot (k \nabla T) + \rho H + \frac{Di_S}{Ra} \underline{\underline{\sigma}} : \underline{\underline{\dot{\varepsilon}}} \tag{3}$$

The variables are total temperature T, composition C, velocity $\underline{v}$ and pressure p. $\underline{\underline{\sigma}}$ is the deviatoric stress tensor and $\underline{\underline{\dot{\varepsilon}}}$ is the strain rate tensor. The governing parameters are Rayleigh number Ra, internal heating rate H, and the surface dissipation number Di_S. Material properties are density ρ, thermal expansivity α, thermal conductivity k, specific heat capacity C_p, and $\Delta\rho_{th} = \alpha\Delta T$, $\Delta\rho_{model} = \rho_{model}(T_{ref}, p) - \rho_{model}(T, p)$, and the density difference is not relied on approximations.

The numerical model is similar to that of *Li et al.* [2015]. All calculations are performed in 2-D spherical annulus geometry with radial and lateral resolutions of 128 and 1024 cells, respectively. The composition field is tracked by about 4 million tracers, and varies between 0 for regular mantle material and 1 for primordial dense material.

We consider a viscosity depending on temperature, depth, yield stress, and post-perovskite (pPv) phase change. We further imposed a viscosity jump of 30 between upper and lower mantles. The viscosity is therefore given by

$$\eta_b(z, T, \Gamma_{pPv}) = \eta_0[1 + 29H(z - 660)] \exp[\Gamma_{pPv} ln(\Delta\eta_{pPv}) + V_a \frac{z}{D} + E_a \frac{\Delta T_S}{(T + T_{off})}]$$
$$\eta_Y = \frac{\sigma_0 + \sigma_i P}{2\dot{e}} \tag{4}$$

$$\eta = \frac{1}{(\frac{1}{\eta_b(z,T,\Gamma_{pPv})} + \frac{1}{\eta_Y})}$$

where η_0 is the reference viscosity (taken at temperature T=1600 K and depth z=0 km), H the Heaviside step function, D the thickness of the mantle, ΔT_S the super-adiabatic temperature difference, and $\Delta\eta_{pPv}$ the viscosity jump between perovskite and post-perovskite. V_a and E_a non-dimensional parameters modeling the activation volume and activation energy, modelling viscosity variations with depth and temperature, respectively, and T_{off} is an offset temperature that reduces the viscosity jump through the top thermal boundary layer. In all our calculations, the value of this parameter is set to $0.88\Delta T_S$. The yield stress helps to build plate-like behavior at the top of the domain. Here, we defined the yield stress by imposing its surface value σ_0, and its pressure gradient σ_i. The yield viscosity η_Y, is defined as the ratio between the yield stress and the second invariant of the strain rate tensor $\dot{e}$. The pPv phase change is determined by a phase function approach following *Christensen and Yuen* [1985]. To avoid numerical difficulties, the viscosity is truncated between 10^{-3} and 10^5 of the reference viscosity.

The reference Rayleigh number is defined as:

$$Ra_{ref} = \frac{\alpha_s g \rho_s \Delta T_S D^3}{\eta_0 \kappa_s} \tag{5}$$

where α_s is the surface thermal expansivity, g the acceleration of gravity, and κ_s the surface thermal diffusivity. This reference Rayleigh number is fixed to 10^8 in all experiments.

The primordial material is set to be denser than the regular mantle material, and the density contrast between primordial and regular mantle materials is controlled by the buoyancy ratio (B) defined as:

$$B = \frac{\Delta\rho_C}{\alpha_s \rho_s \Delta T_S} \tag{6}$$

where $\Delta\rho_C$ is the density difference between the dense and regular materials. The buoyancy ratio is varied between 0.18 and 0.26 in order to explore different stability states for the large primordial reservoirs. For a superadiabatic temperature difference $\Delta T_S = 2500$ K and thermal expansion $\alpha_s = 5.0 \times 10^{-5}$ K^{-1}(taken at $z = 0$ and $T = 1600$ K), B=0.26 leads to a density contrast of 100 kg/m^3, corresponding to a relative density anomaly of about 2% at the bottom of the mantle. This value is in agreement with estimates of chemical density anomalies in the lowermost mantle from probabilistic tomography [e.g., *Trampert et al.*, 2004; *Mosca et al.*, 2012]. The initial temperature consists in an adiabatic 1-D profile with a potential temperature of 2000 K and thermal boundary layers at top and bottom (the temperature is fixed to 300 K at the top and 3750 K at the CMB), to which random perturbations are added. The shell is heated from both the bottom and within. The initial thickness of the primordial layer is 0.07, equivalent to 5% of the total mantle volume. The values of other physical parameters are chosen to provide the best possible description of mantle convection, as determined by systematic searches [*Li et al.*, 2014a, 2015], and are listed in Table S1.

References

Christensen, U. R., and D. A. Yuen (1985), Layered convection induced by phase transitions, *Journal of Geophysical Research*, *90*, 10291 – 10300.

Li, Y., F. Deschamps, and P. J. Tackley (2014a), The stability and structure of primordial reservoirs in the lower mantle: insights from models of thermochemical convection in three-dimensional spherical geometry, *Geophysical Journal International*, *199*(2), 914–930, doi:10.1093/gji/ggu295.

Li, Y., F. Deschamps, and P. J. Tackley (2015), Effects of the post-perovskite phase transition properties on the stability and structure of primordial reservoirs in the lower mantle of the earth, *Earth and Planetary Science Letters*, *432*, 1 – 12, doi: 10.1016/j.epsl.2015.09.040.

Mosca, I., L. Cobden, A. Deuss, J. Ritsema, and J. Trampert (2012), Seismic and mineralogical structures of the lower mantle from probabilistic tomography, *Journal of Geophysical Research: Solid Earth*, *117*(B6), doi:10.1029/2011JB008851.

Tackley, P. J. (2008), Modelling compressible mantle convection with large viscosity contrasts in a three-dimensional spherical shell using the yin-yang grid, *Physics of the Earth and Planetary Interiors*, *171*(1-4), 7 – 18, doi:10.1016/j.pepi.2008.08.005.

Trampert, J., F. Deschamps, J. Resovsky, and D. Yuen (2004), Probabilistic tomography maps chemical heterogeneities throughout the lower mantle, *Science*, *306*(5697), 853–856, doi:10.1126/science.1101996.

Vilella, K., S.-H. Shim, C. G. Farnetani, and J. Badro (2015), Spin state transition and partitioning of iron: Effects on mantle dynamics, *Earth and Planetary Science Letters*, *417*, 57–66.

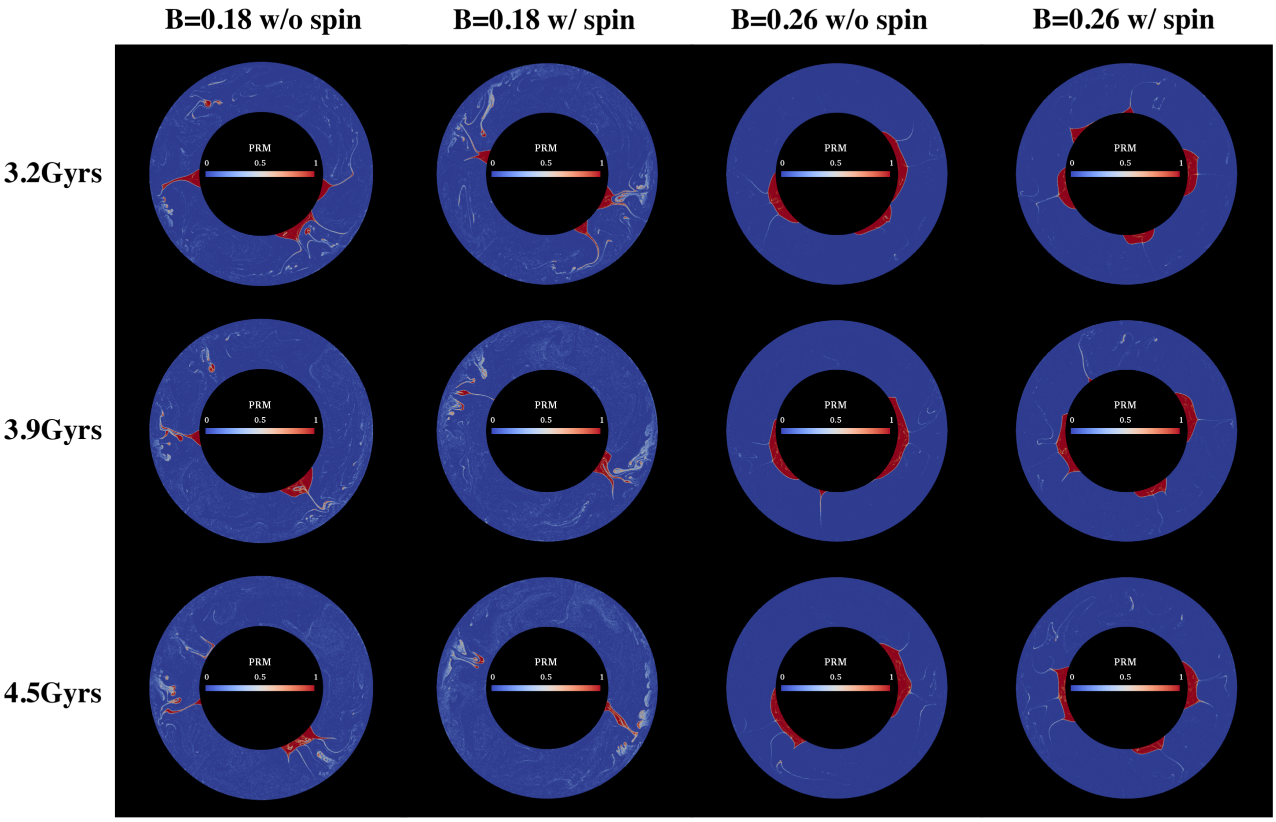

Figure 1. Snapshots of evolution of composition fields for B=0.18 and B=0.26 with/without iron spin transition. Snapshots time are t=3.2, 3.9, 4.5 Gyrs from top to bottom.

Table 1. Table S1. Parameters of the numerical models

Parameter	Symbol	Value
Acceleration of gravity	g	9.81 m s^{-2}
Mantle thickness	D	2891 km
Super-adiabatic temperature difference	ΔT_S	2500 K
Reference adiabatic temperature	T_{as}	1600 K
Surface density	ρ_S	3300 kg/m^3
CMB density	ρ_b	5500 kg/m^3
Surface thermal expansion	α_S	5.0×10^{-5} K^{-1}
CMB thermal expansion	α_b	1.0×10^{-5} K^{-1}
Surface thermal diffusivity	κ_S	6.24×10^{-7} m^2s^{-1}
CMB thermal diffusivity	κ_b	8.74×10^{-7} m^2s^{-1}
Clapeyron slope at z=660km	Γ_{660}	-2.5 MPa/K
Reference thermal viscosity	η_0	1.6×10^{21} Pa s
Viscosity ratio at z=660km	η_{660}	30
Thermal viscosity ratio	$\Delta\eta_T$	10^9
Vertical viscosity ratio	$\Delta\eta_Z$	10^2
Viscosity ratio between pv and ppv.	$\Delta\eta_{ppv}$	1